

# A novel face mask design with improved properties for COVID-19 prevention

Laine Alby<sup>1</sup>, Ajay Jayswal<sup>1</sup> , Sarah Morris<sup>2</sup>, Will McAtee<sup>2</sup>,  
 Vrishank Raghav<sup>2</sup> and Sabit Adanur<sup>1</sup> 

## Abstract

Novel cloth face masks to mitigate the spread of COVID-19 have been developed and tested for particle (0.1  $\mu\text{m}$  in size) filtration efficiency, bacterial filtration efficiency, breathability, leakage, heart rate, and blood oxygen level, and then compared with the available N95 masks and surgical masks. It was found that this novel mask had better filtration efficiency than that of surgical masks and was very close to that of N95 masks. The breathability was also improved and was in the range of the designated levels for barrier face coverings. The flow visualization technique was utilized to study the leakage of the mask and it was found to have significantly lower leakage as compared to surgical masks. Heart rate and blood oxygen level tests were performed by wearing the mask during 10-minute walking sessions and it was found that wearing the mask did not adversely affect heart rate or blood oxygen levels or add any other strain on the wearer. It is believed that this novel face mask would reduce the spread of COVID-19 as well as provide an environmentally and economically conscious alternative to the N95 respirators for the public. The mask developed in this study can be washed, reused, and therefore worn for longer periods of time.

## Keywords

Face masks, COVID-19, bacterial filtration efficiency, breathability, flow visualization

## Introduction

The nation is going through an unprecedented time due to the coronavirus pandemic. The Center for Disease Control and Prevention (CDC) has promoted the use of face masks in crowds or gatherings to combat the swift spread of this disease.<sup>1</sup> The CDC also denoted loose-fitting fabric face coverings as the least effective form of protection, with tightly-fitting and National Institute for Occupational Safety and Health (NIOSH)-approved respirators such as N95 masks as the most effective. Although N95 masks have been proven to be the most effective form of face covering in reducing viral transmission,<sup>2</sup> they are not recommended to be worn for long periods of time and are not as effective once reused.<sup>3</sup> Constructing and producing a mask design that is effective, reusable, and comfortable could decrease the transmission of this devastating virus. The world has suffered huge losses from the pandemic to date and pursuing methods of decreasing the power of this virus will only have positive repercussions. Considering the limited resources and strain placed on the production of masks during

a worldwide pandemic, constructing a mask that can be replicated at home and reused many times is a vital part of design considerations for a novel mask.

Fibrous filters prevent the flow of contaminants in multiple ways. Fibrous filters are defined as simple, economical devices that are capable of removing sub-micrometer particles from gas streams, a benefit which is particularly useful in medical products such as face coverings or respirators. Because of the very small size of the particles in question, various parameters can affect performance of these filters including particle shape, aggregate morphology, flow regime, humidity, fiber size, and particle loading.<sup>4</sup> Porosity is an important parameter in regulating the collection efficiency

<sup>1</sup>Department of Mechanical Engineering, Auburn University, USA

<sup>2</sup>Department of Aerospace Engineering, Auburn University, USA

## Corresponding author:

Sabit Adanur, Department of Mechanical Engineering, Auburn University, 1418 Wiggins Hall, Auburn, AL 36849, USA.

Email: [adanusa@auburn.edu](mailto:adanusa@auburn.edu)

that is intended. Porosity is defined as the total volume of air over the fabric volume and decreasing the porosity of the material increases the filter performance, but doing so requires more back pressure to ensure the same flow rate through the filter.<sup>5</sup>

An ideal fibrous filter has a high collection efficiency value and a low pressure drop value. Collection efficiency is often a function of particle size, and it is defined as the fraction of entering particles that are collected by the filter. The parameters investigated in this project that reflect on this idea are bacterial filtration efficiency and initial filtration efficiency. For high-efficiency filters, as the mask for this work is intended to be, penetration is a helpful indicator as well, which is defined as one minus the collection efficiency.<sup>6</sup> To construct this value, various capture mechanisms are at work. Particles may deposit on a fiber through inertial impaction, interception, Brownian motion, gravitational settling, and electrostatic forces.<sup>5</sup>

Inertial impaction occurs when a particle departs from its original gas streamline and hits a fiber, thereby not passing through the filter material. Interception occurs because particles have finite size, and when the particle comes within one particle radius of the fiber surface, deposition occurs even if it remains on its original gas streamline. Brownian motion, or random motion of small particles suspended in fluid, can be sufficiently strong enough to divert a particle from its streamline and into a fiber. Gravitational settling can contribute to filtration capture, but this effect is often negligible for nanoparticles due to their small size and mass. Electrostatic forces occur when fibers carry electric charges, which can polarize fibers and cause charged particles to divert towards fibers.<sup>7</sup>

Since the beginning of the COVID-19 outbreak, several studies have been performed on the filtration performance of improvised mask materials as well as current mask materials, but mostly in ideal-fit scenarios. However, these masks may not provide the correct performance measures when the face covering is worn, including gaps and issues with fit. This can give the user a false impression of the level of protection they have from COVID-19 transmission when wearing the covering in a high-risk environment.<sup>8</sup>

Various studies have investigated fit modifications that can help reduce leakage and retain the base level of filtration efficiency of the mask material. A research team at Northeastern University investigated the effect of adding a nylon overlayer to surgical-style masks and other homemade cloth masks on the filtration efficiency of the design by utilizing an abridged testing process that can allow for quicker testing of mask compositions during the pandemic.<sup>9</sup> This study concluded that the fit of cotton face masks is variable depending on fit and quality of materials, but that fit is an important factor

in the use of all masks, ranging from N95 masks to surgical masks. A poorly fitted and a well fitted N95 mask exhibited a mean particle removal efficiency of 90.6% and 99%, respectively. A standard medical-type mask without and with the nylon overlay showed a mean particle removal efficiency of 50–75% and 86–90%, respectively.<sup>9</sup>

Finally, some studies have implemented fit modifications to existing mask designs to evaluate the effect these have on eliminating gaps. A fit factor assessment was performed before and after applying various fit modifications to source control masks. The most effective fit modification to the surgical masks tested was the addition of a brace, which increased the human fit factor of medical masks by at least six times the original fit factor, and it increased the fit factor of each cloth mask as well.<sup>10</sup> However, a rigid brace-like structure was determined to be the most effective addition to the mask to improve fit in our design.

To construct a well-performing face covering, fabric selection is an integral part of the design that affects its filtration capabilities, especially when an inner filter layer is not considered. For that reason, various studies were investigated regarding the capabilities of commonly available fabrics and their performance in filtration and breathability for the application of constructing face masks. Since the pandemic started, some research groups have investigated this topic to address the limited availability of traditionally used face mask and filtration materials. The strain placed on providing medical-grade face coverings limited the availability to the public, causing them to utilize fabrics available in their own homes. Constructing a mask from commonly available textiles would give users the ability to make their own effective mask at home if necessary.

Standard mask testing methods, consisting of American Society for Testing and Materials (ASTM) F2101-14, using the model virus bacteriophage MS2 were used to test the viral filtration efficiency of various fabric masks as well as commercially available disposable, surgical, and N95 masks.<sup>11</sup> Of the fabric masks, one included a pocket filter, which was tested without a filter, with a dried baby wipe, and with a section of a vacuum cleaner bag. The test results concluded that the best performing mask was the pocket filter mask, composed of cotton, when it contained the vacuum bag section as its filter medium. With an aerosol size of 6  $\mu\text{m}$ , the viral filtration efficiency was 99.5%, and with an aerosol size of 2.6 micrometers the filtration efficiency was 98.8%. These values are both very close to the advertised efficiency of surgical masks. However, the most important element of this efficiency value is proper fit, which was not explored in that study.

In another study, 15 types of natural and synthetic fabrics were used to construct masks of either single

layers, double layers of the same fabric, or a combination of multiple fabrics to determine filtration efficiency.<sup>12</sup> The most thoroughly investigated fabric is cotton, in which various thread-per-inch (TPI) values were tested in different layers. Lower TPI cotton (80 TPI) performed much worse than higher TPI cotton (600 TPI). However, it is noted that improper fit can reduce the efficiency of the mask by up to 50%. Therefore, ensuring proper sealing of the mask is vital to retaining good filtration efficiency values. It is also important to note that the two-layer cotton design produced a mask with a high filter efficiency, especially above 300 nm at 99.5%. The pressure differential exhibited by this combination was 2.5, which lies in the middle of the range of the combinations tested.

One of the aims of this research is to utilize 100% cotton plain woven fabric with a meltblown insert to manufacture a face mask and overcome the shortages in the surgical, and other cloth masks available in the market. The fabric composition is tested for particles (0.1  $\mu\text{m}$  in size) filtration efficiency, bacterial filtration efficiency (BFE), breathability, leakages and fit.

## Materials and methods

### Fabric selection

Figure 1 shows the components of a novel face mask designed during this work. It contains a nose brace piece, mouth brace piece, mask body, and a removable meltblown filter insert. A plain woven 100% cotton fabric was utilized for the mask body as shown in Figure 2, along with its pore size distribution. The average pore size is  $5.05 \pm 0.41 \mu\text{m}$ . This fabric had a yarn density of 28 yarns/cm and a weight of 412 grams per square meter (GSM). Figure 3 shows the magnified picture of the Polypropylene (PP) meltblown insert.

The filter has an average pore size of  $2.90 \pm 0.14 \mu\text{m}$ , average thickness of 0.198 mm, and the weight of 34.5 GSM. The pore size distributions were determined using ImageJ and OriginPro software.

### Manufacturing of the face masks

The inner filter layer consists of one layer of meltblown filter material in the shape of the filter pocket of the mask. The mask incorporates two channels in which 3D printed brace sections are inserted to improve the seal along the nose bridge as well as to keep the fabric from touching the user's mouth during use, which are shown in Figure 4.

The mask design includes ear loops which, when not worn, retract close to the mask body to prevent them from catching on objects when in a pocket or bag, which is accomplished by extending the fabric of the mask outwards towards the ears. Doing this also reduces leakage on the sides of the mask, thereby increasing its filtration capabilities. The ear loops in their unused, retracted form are shown in Figure 1, while Figure 5 demonstrates the mask as it would be during use.

The fabric mask body was sewn using a Singer Heavy Duty 4432 Sewing Machine, and polylactic acid (PLA) brace pieces were 3D printed using the (Figure 6). The nose piece was printed first as a flat rectangular prism, and then it was heated by the 3D printer bed to a temperature of 70°C, which is near the glass transition temperature of PLA, where it becomes flexible. The nose piece is then formed to the user's nose contour exactly by placing the flexible brace against the nose contour until it has cooled and hardened. The mouth brace piece is printed at a contour initially and does not need to be bent.



**Figure 1.** Novel face mask components, including (a) the nosepiece, (b) the mouthpiece, (c) the mask body, and (d) removable meltblown insert.

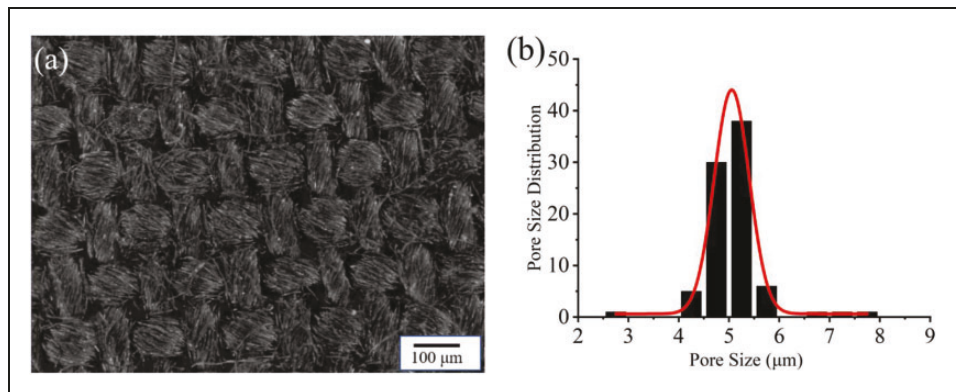


**Figure 2.** (a) Optical microscope image of plain-weave cotton fabric and (b) pore size distribution of plain weave cotton fabric.

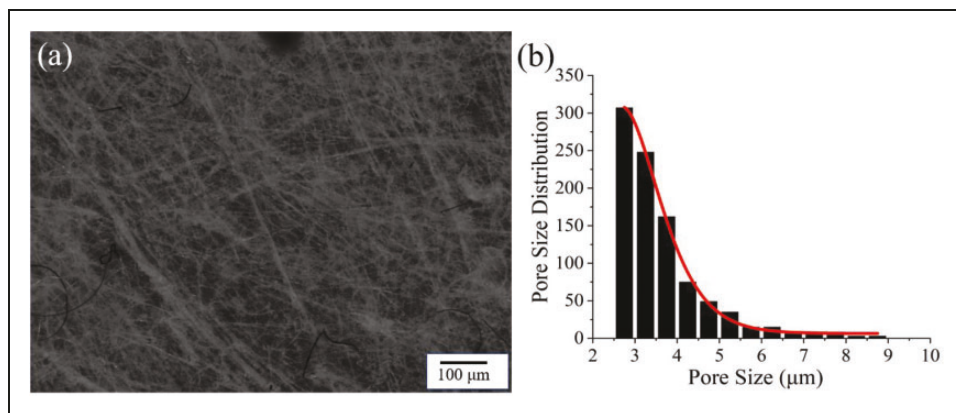


**Figure 3.** (a) Optical microscope image of meltblown polypropylene (PP) filter insert and (b) pore size distribution of meltblown filter insert.

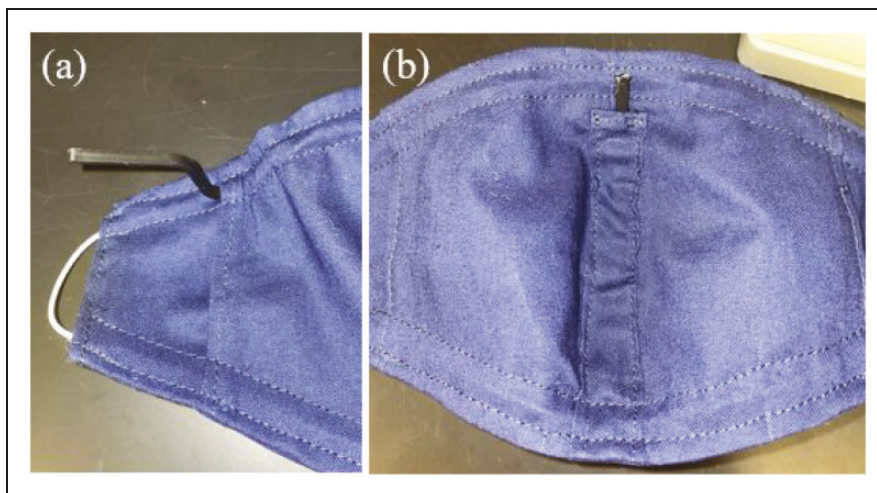


**Figure 4.** Mask design and fabrication showing the brace insert channels. (a) Nose brace piece and (b) mouth brace piece.

After design and fabrication of the face mask, a silver nanoparticle coating was added to the outermost layer of fabric to reduce bacterial contamination. HeiQ HyProTecht is a stable, broad-spectrum biocide

intended for use in the manufacture of polymers and coatings for textiles. It demonstrates a strong antimicrobial efficacy, and the coating is effective once applied for at least 30 washes at 140°F. To apply the



**Figure 5.** Face mask fabricated during this work. (a) Front view and (b) side view.

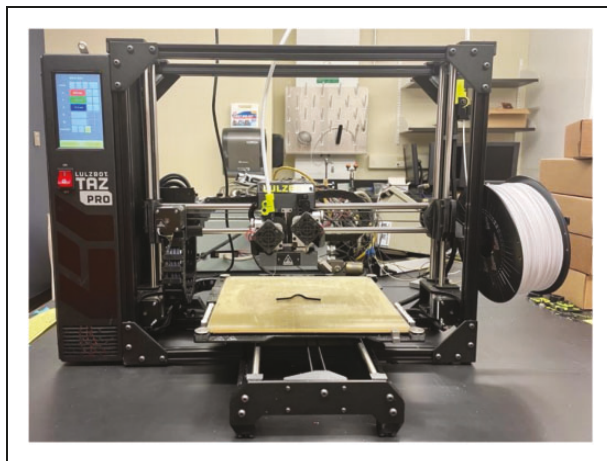


**Figure 6.** Lulzbot TAZ Pro 3D printer printing polylactic acid (PLA) brace.

coating, the material must be atomized. The atomization process was accomplished using a broadband ultrasonic generator and an ultrasonic nozzle. An automated dispensing machine was programmed using a teach pendant to dispense an even square of the coating onto two pieces of fabric that were used to construct the outside of the mask design. The setup is shown in Figure 7.

#### Testing of the face masks

**Fabric testing.** Different types of tests were conducted to evaluate the effectiveness of the fabric being used in the project. The mask consists of outer layers made of

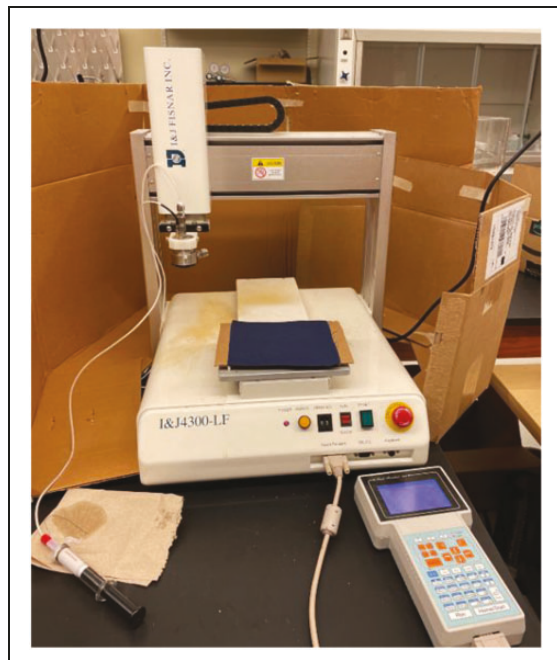


**Figure 7.** Automated dispensing robot and teach pendant setup for dispensing HeiQ HyProTecht coating onto fabric.

plain weave cotton fabric and the inner layer made of meltblown filter material.

The ASTM F2299/F2299M-03 test method was used to measure the initial particle filtration efficiency of materials used in the medical facemasks by using monodispersed aerosol. Particle counting was performed by light scattering in the range of 0.1–5.0  $\mu\text{m}$ ,

using airflow velocities in the range of 0.5–25 cm/s.<sup>13</sup> The aerosol filtration efficiency of a particular particle size is determined by equation (1).

$$\eta(D_p) = [1 - P(D_p)] \times 100 \quad (1)$$

where,  $P$  represents the penetration,  $D_p$  represents the particle size, and  $\eta$  represents the downstream particle concentration divided by the upstream particle concentration. This calculated value is then used to compare the efficiencies of the medical face mask materials.

The test method EN14683:2019 Annex C for medical face masks was used to determine breathability, which is measured by differential pressure. The differential pressure that is required to draw air through a surface area at a constant flow rate is the air exchange pressure of the mask material used in testing.<sup>14</sup> The mask was attached between two sample holders with a circular cross-section of 4.9 cm<sup>2</sup>, and air passed through the mask at a fixed airflow rate of 81/min. The breathing resistance was calculated by measuring the differential pressure drop ( $\Delta P$ ) across the mask material, which is calculated using equation (2) and expressed in Pa/cm<sup>2</sup>.

$$\Delta P = \frac{X_{m1} - X_{m2}}{A} \quad (2)$$

where  $X_{m1}$  represents the lower pressure side of the material,  $X_{m2}$  represents the higher-pressure side, and  $A$  is the cross-section of the test material.

The ASTM F2101-19 standard test method was used to evaluate the BFE of the medical face mask materials, using the biological aerosol, *Staphylococcus aureus*. This test method uses a ratio of the upstream bacterial challenge to the downstream residual concentration to determine filtration efficiency of medical face mask materials. The BFE was calculated using equation (3).

$$BFE = \left( 1 - \frac{T}{C} \right) \times 100\% \quad (3)$$

where,  $BFE$  is the filtration efficiency,  $T$  is the plate count total for the test sample, and  $C$  is the average plate count total for the test controls.<sup>15</sup>

To assess the effectiveness of masks, BFE and  $\Delta P$  are used to define a comprehensive filtration quality factor, which allows for a more robust comparison among filtration media.<sup>16</sup> The quality factor (QF) is determined by using equation (4):<sup>17</sup>

$$QF = \frac{-\ln(1 - BFE)}{A \times \Delta P} \quad (4)$$

where,  $A$  is the cross-section area (4.9 cm<sup>2</sup>) of the test material.

**Flow visualization.** The mask design was further analyzed by imaging the flow leakage around the mask for a single-pulsed cough. The leakage of the current mask design was compared to that of the commonly used surgical face masks. A custom-built pulsatile coughing simulator was used for these tests, as shown in Figure 8. The simulator utilizes a solenoid valve that is run by a National Instruments (NI) DAQ to control the flow duration. At the wall, a flow regulator controls the air flow rate. This air then runs to an in-line pressure relief chamber to smooth the flow profile to mimic that of a natural cough. The outlet pipe of the simulator has a diameter  $D = 2.54$  cm, with length  $L/D = 40$  to ensure fully developed flow. A mannequin face with a corresponding outlet was placed at the end of the pipe in order to fit the mask to the face. The nose piece was formed against the mannequin face to ensure the best fit.

The flow leakage of the face mask was compared with that of a surgical mask using this setup with a single-pulsed cough duration of  $T_1 = 0.225$  s and cough peak flow rate of 4.51/s. The flow leakage was measured in two planes: the sagittal plane for leakage along the nose bridge, and a slightly angled transverse plane to illuminate side leakage, extending through both the mouth and ear of the mannequin as shown in Figure 9. The flow leakage was made visible by smoke flow visualization. The outlet pipe was filled with smoke from a fog machine prior to experiments

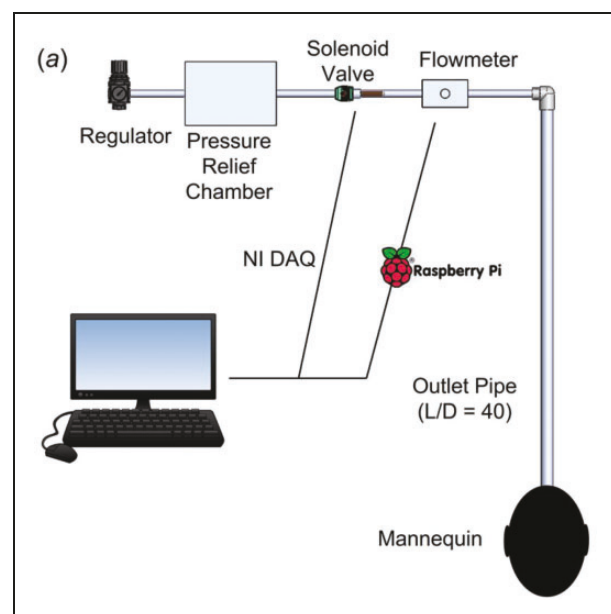


**Figure 8.** Laser illumination testing setup and configuration for cough simulation.<sup>18</sup>

such that it was expelled through the cough. A 532 nm continuous-wave laser was used to illuminate the flow leakage in the sagittal plane and side plane by converting the laser beam to a light sheet. The leakage was captured at 30 fps using a Nikon Z50 mirrorless camera.

**Performance testing.** To test the performance of the masks, and to evaluate the performance effects of the silver nanoparticle coating, three tests were performed in which the mask was worn during 10-minute walking sessions, and the average value was reported. Heartbeat rates and blood oxygen percentages were recorded throughout each session. The experiment was conducted while wearing no mask, wearing the mask without the silver coating, as well as wearing the mask with the silver coating. The same nosepiece and mouthpiece were used for each design. Additionally, the same pattern and dimensions were used to produce each tested mask.

## Results and discussions

### Fabric test results

The test results for the initial efficiency of the fabrics are shown in Table 1, which gives an average initial

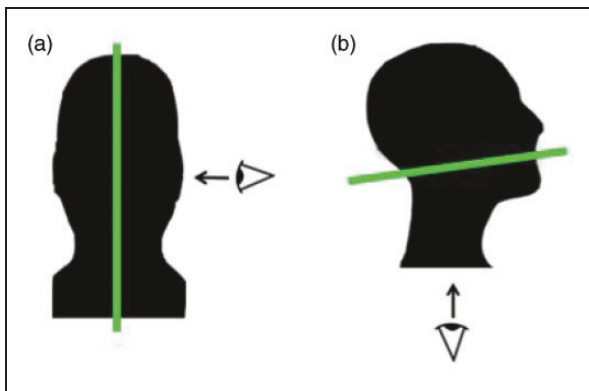


**Figure 9.** (a) Sagittal plane positioning of laser with camera positioned beside mannequin and facing the plane to capture leakage along the nose bridge and (b) side plane positioning of laser with camera facing plane from underneath mannequin head to capture leakage on the sides of face covering.<sup>18</sup>

**Table 1.** Initial particle filtration efficiency test results with 0.1  $\mu\text{m}$  particles (mean  $\pm$  standard error)

Filter ID	Differential pressure (mm H <sub>2</sub> O)	Port	Particles (0.1 $\mu\text{m}$ )	Efficiency (%)	Conditions
24,798	8.34 $\pm$ 0.14	Upstream Downstream	203586 $\pm$ 557.82 52505 $\pm$ 4536.20	73.69 $\pm$ 2.19	Temp: 21.1 $\pm$ 0.17°C RH: 40.38 $\pm$ 0.70% BP: 728 mm Hg

BP: barometric pressure; RH: relative humidity.

Note: This test was done five times and the average value is reported.

efficiency of 73.69% out of five tests. Initial efficiency values were calculated using latex microspheres having a particle size of 0.1  $\mu\text{m}$ . Filter ID is the name of the sample given by the third party who conducted the tests for identification purposes.

A surgical mask is designed to prevent the large-particle droplets, splashes, sprays, or splatter with a diameter of  $>100\text{ }\mu\text{m}$  from reaching the mouth and nose. A surgical mask cannot prevent inhalation of very small particles present in the air and hence it does not provide complete protection against germs and other contaminants.<sup>19</sup> On the other hand, the filtration efficiency of N95 masks for particles smaller than 0.3  $\mu\text{m}$  is around 85% due to its wider pore size (300 nm).<sup>20</sup> The viruses of 0.3  $\mu\text{m}$  size are easier to filter than those that are larger than 0.3  $\mu\text{m}$ , because 0.3  $\mu\text{m}$  particles follow a Brownian motion (random, zigzag) and therefore trap more easily into filters by diffusion mechanism.<sup>21</sup> The severe acute respiratory syndrome coronavirus-2 (SARS-CoV-2 virus) is essentially spherical, albeit slightly pleomorphic, with a diameter of 0.06–0.14  $\mu\text{m}$ .<sup>2,22–24</sup>

The face mask developed in this study has better particle filtration efficiency than surgical face masks. While comparing with that of a N95 mask, which has a filtration efficiency of about 85% for particles below 0.3  $\mu\text{m}$ , the filtration efficiency of this mask (about 74% for particles of 0.1  $\mu\text{m}$ ) is quite impressive. It should also be noted that the particles smaller than 0.3  $\mu\text{m}$  in size follow a Brownian motion and can get trapped easily by the filters by diffusion mechanism. With all these arguments, it can be said that this mask has better filtration efficiency and can be used for protection against COVID-19.

A breathability test was conducted on the fabric composition. In this test, the measurement area indicates a different section of the sample that was set in the testing ring for each iteration. The differential pressures measured of all five samples was averaged. This test was performed for the mask design without the addition of the HeiQ HyProTech coating in SGS IBR Laboratories in Grass Lake, Michigan, USA.

The breathability or differential pressure test results are shown in Table 2, which shows an average

**Table 2.** Results of the EN14683:2019 Annex C Method for determination of breathability (differential pressure) (mean  $\pm$  standard error)

Filter ID	Measurement areas	Mean differential pressure (mm H <sub>2</sub> O)	Mean differential pressure/area (mm H <sub>2</sub> O/cm <sup>2</sup> )	Conditions
24,798	5	24.64 $\pm$ 0.64	5.02 $\pm$ 0.13	Temp: 23.08 $\pm$ 0.02°C RH: 37.68 $\pm$ 0.40% BP: 727.9 mm Hg

Note: This test was done five times and the average values are reported.

differential pressure of 5.02 mm H<sub>2</sub>O/cm<sup>2</sup>. This breathability value comes at slightly below that of N95 respirator, but about twice the value of surgical masks, indicating that the mask is less breathable than surgical masks but not as difficult as N95 masks. An N95 respirator has an average differential pressure of 5.5 mm H<sub>2</sub>O/cm<sup>2</sup>, while a surgical mask has an average differential pressure of 2.24 mm H<sub>2</sub>O/cm<sup>2</sup>.<sup>1</sup> According to the ASTM F2100-11 protocol, the differential pressure value should be at minimum less than 5.0 mm H<sub>2</sub>O/cm<sup>2</sup>. Therefore, the mask constructed sits right at this desired value. Often, N95 masks have differential pressure values that surpass this, and surgical masks are generally much lower.

A BFE test was performed using air at a flow rate of 81/min and with a standard effective area of 4.9 cm<sup>2</sup>. The set-up parameters are shown in Table 3. In this test, the plate count represents the number of test bacteria counted on the sample at the end of the testing period. The colony forming unit (CFU) is a measurement unit used to demonstrate visible agar colonies on a test sample. The test results are shown in Table 4. The test specimens for BFE testing were conditioned for a minimum of 4 h prior to testing. Temperature was maintained at 21  $\pm$  5°C, relative humidity was maintained at 85  $\pm$  5%, and stages correlate to the six-stage viable particle cascade impactor. This test was performed for the mask design without the addition of the HeiQ HyProTecht coating.

The BFE test results indicate a very high average efficiency value of 99.31% at the particle size of 3.3  $\mu$ m for the tested agent, *Staphylococcus aureus*. In comparison, the mean particle size of COVID-19 has been shown to vary between 0.06–0.14  $\mu$ m.<sup>2,22–24</sup> It is also important to consider that the virus is transmitted through respiratory droplets, which are larger than the mean particle size of coronavirus alone and are typically 5–10  $\mu$ m in length. This is much higher than the size of the *Staphylococcus aureus* particles tested, suggesting that the filtration efficiency of larger respiratory particles is very high for the face mask designed. It was reported that the average BFE of an N95 mask is 99.9%, while surgical masks had an average BFE of 97.48%.<sup>25</sup> Therefore, the mask tested had a BFE very

**Table 3.** ASTM F2101 testing conditions for bacteria filtration efficiency (BFE) testing by SGS IBR Laboratories

Challenge	<i>Staphylococcus aureus</i>
Area of test specimen (cm <sup>2</sup> )	48.3
Specimen side facing challenge	Inside
Flow rate (lpm)	28.3
Mean particle size (MPS) of challenge aerosol ( $\mu$ m)	3.3
Average plate count of positive control	2239 CFU
Plate count of negative control	0 CFU

CFU: colony forming unit; PP: Polypropylene SGS IBR is the name of laboratory where the testings were done.

**Table 4.** ASTM F2101 test data from bacteria filtration efficiency (BFE) test

Sample tested	Results (CFU)				
	1	2	3	4	5
Stage 1	0	1	1	0	0
Stage 2	0	0	0	0	0
Stage 3	0	0	0	1	1
Stage 4	1	1	2	0	0
Stage 5	14	12	17	1	13
Plate count total	17	21	22	2	15
% BFE	99.24%	99.06%	99.02%	99.91%	99.33%
Average % BFE	99.31 %				

CFU: colony forming unit.

close to that of the N95 mask and much higher than that of the surgical masks tested.

By combining the BFE and differential pressure, the desired functions of a face mask such as comfort and high filtration ability can be represented by a single value. Masks having lower differential pressure and higher BFE are considered to be the best masks.<sup>26</sup> The quality factor (QF) of our face mask is found to be 0.2023 Pa<sup>-1</sup>, which shows that it has good filtration qualities. To improve the QF, differential pressure needs to be lowered without compromising the filtration efficiency. Often, a compromise has to be made between the BFE and the breathability to manufacture the face masks with acceptable properties. For the masks designed, the differential pressure falls under

the ASTM F2100-11 protocol for normal breathing. Hence, it can be said that a better filtration efficiency with designated breathability has been achieved.

### Flow visualization results

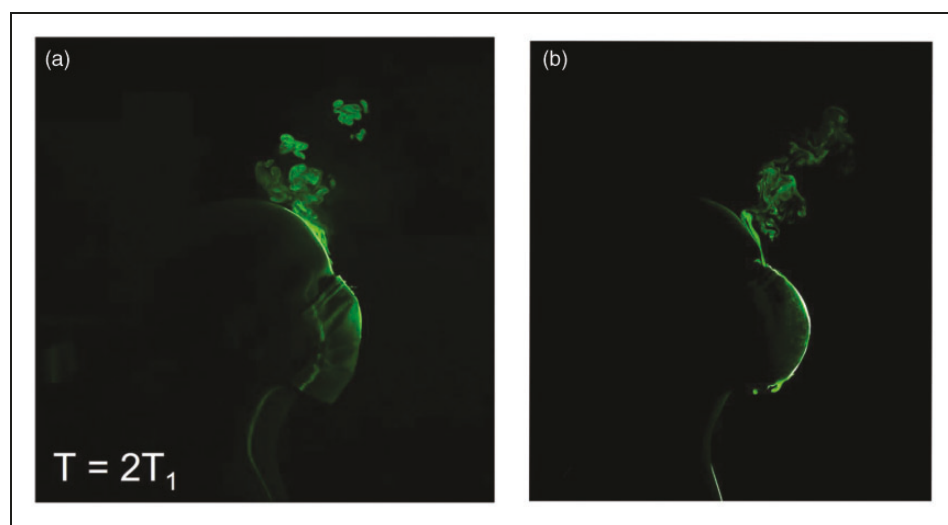
The flow visualization results are shown in Figures 10 and 11. Figure 10 shows the leakage flow in the sagittal plane at the top of both the surgical and the current mask. At the same time ( $T = 2T_1$ ), there appears to be less flow leakage at the top of the current mask design.

Figure 11 shows the leakage flow at the side of the mask. In this plane, there is a clear difference in the amount of flow leakage between the surgical and the current mask. Significant leakage can be observed around the surgical mask. In contrast, very little flow leakage can be seen at the side of the current mask. This is attributed to the extension of fabric toward the ears in the current mask design, as described in the section above on manufacturing of the face masks. As a result of this extension, the side opening of the mask is significantly reduced in length compared

to a surgical mask and is also further away from the mouth opening. This test showed that the current mask has better performance in terms of leakage.

### Performance test results

Figure 12 demonstrates the results of all performance tests, which shows that the heartbeat rate remained within a range of 98–102 beats per minute (BPM) and the blood oxygen level varied in the range of 96–100% throughout the experiments. The 10-minute walk at a speed of 3 miles/h (4.8 km/h) while wearing the mask with silver nanoparticle coating resulted in an average heartbeat rate of 98 BPM and the blood oxygen level increased from 96% before the test to 100% after the test. Wearing the mask without coating resulted in an average heartbeat rate of 102 BPM and the blood oxygen level changed from 100% before the test to 99% after the test. Similarly, the test performed without wearing a mask had an average heartbeat rate of 101 BPM, which is only 1 BPM lower than that of the test performed while wearing the uncoated mask.



**Figure 10.** Smoke flow visualization of leakage along the sagittal plane for (a) surgical mask and (b) current mask.

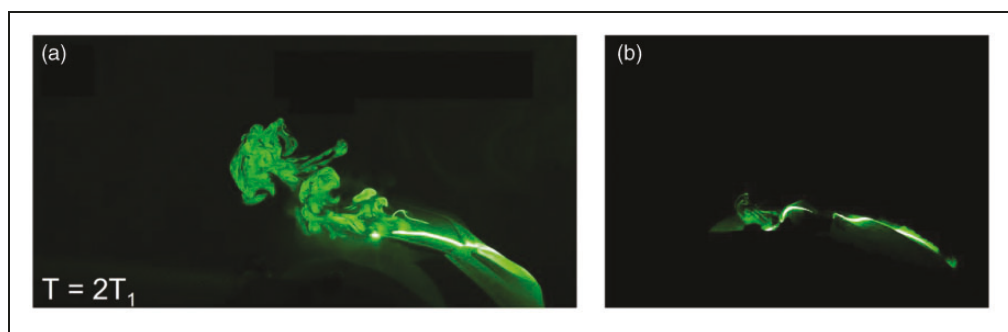


**Figure 11.** Smoke flow visualization of leakage along the side plane: (a) surgical mask and (b) current mask.

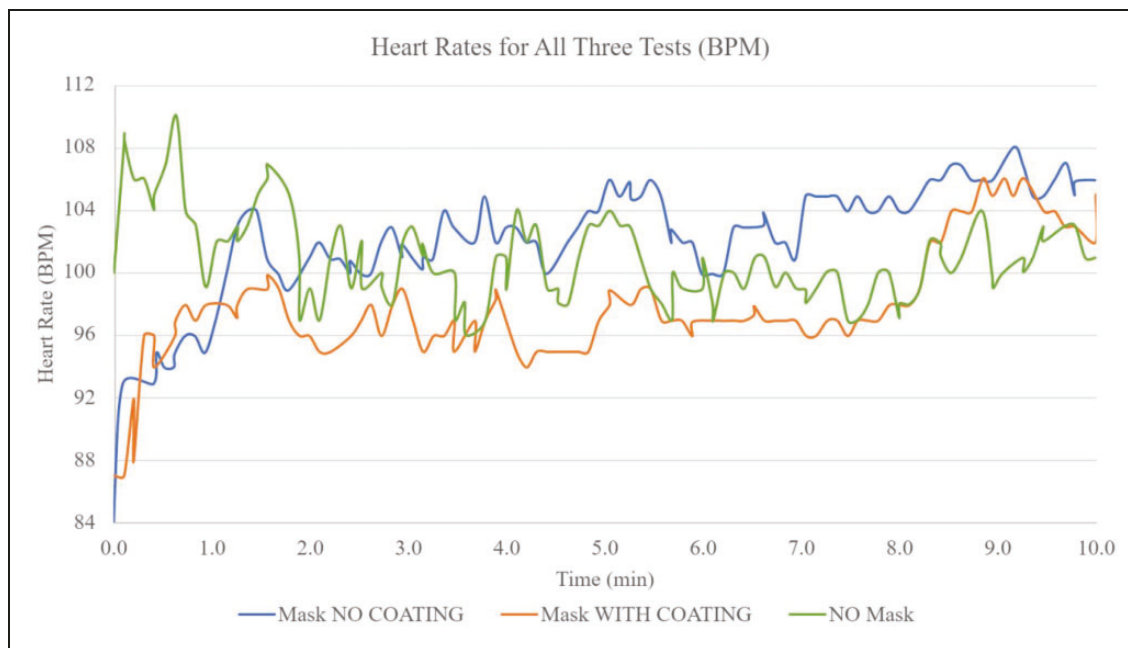


**Figure 12.** Comparison of heartbeat rates during a light exercise.

The initial blood oxygen level reported before the test was 99%, while the blood oxygen after the test was 97%. Thus, these tests showed similar heartbeat rates and blood oxygen levels. Hence, it can be said that the wearing of the new face mask with or without silver nanoparticle does not have much effect on heartbeat rate and blood oxygen level. Therefore, it should not cause the wearer added strain during light exercise, talking or breathing and can be useful to prevent the spread of contagious viruses and bacteria.

## Conclusions

A novel cloth face mask has been designed and produced with improved filtration efficiency, better leakage prevention on a sagittal and side plane, and no significant effect on heart rates and blood oxygen levels during light exercise and talking. The filtration efficiency of this new face mask is about 74% for particles of  $0.1\text{ }\mu\text{m}$ , which is better than that of surgical masks and is comparable with that of N95 mask which has a filtration efficiency of about 85% for particles below  $0.3\text{ }\mu\text{m}$  in size. The new face mask has a very high BFE level, as well as a differential pressure value close to that of an ASTM certified level 3 barrier face covering, which is the designated level for barrier face coverings. The flow visualization technique revealed that flow leakage is reduced significantly at the top (nose bridge) and side of the current mask design. In addition, it does not adversely affect heart rate or

blood oxygen levels of the wearer during light exercise, talking or regular breathing. With all these features, this mask can be helpful in reducing the spread of contagious diseases like COVID-19.

## Declaration of conflicting interests

The author(s) declared no potential conflicts of interest with respect to the research, authorship, and/or publication of this article.

## Funding

The author(s) disclosed receipt of the following financial support for the research, authorship, and/or publication of this article: The project was made possible by funding from the Alabama Department of Economic and Community Affairs (ADECA), Grant No. 1ARDEF2104, which is appreciated.

## ORCID iDs

Ajay Jayswal  <https://orcid.org/0000-0002-1623-0682>  
Sabit Adanur  <https://orcid.org/0000-0002-5433-3084>

## References

1. Centers for Disease Control and Prevention. Types of masks and respirators, *U.S. Department of Health & Human Services*, <https://www.cdc.gov/coronavirus/2019-ncov/prevent-getting-sick/types-of-masks.html> (2022, accessed 3 August 2022).
2. Kim MC, Bae S, Kim JY, et al. Effectiveness of surgical, KF94, and N95 respirator masks in blocking SARS-CoV-2: A controlled comparison in 7 patients. *Infect Dis (Auckl)* 2020; 52: 908–912.

3. World Health Organization. Rational use of personal protective equipment (PPE) for coronavirus disease (COVID-19), [https://apps.who.int/iris/bitstream/handle/10665/331498/WHO-2019-nCoV-ICPPPE\\_use-2020.2-eng.pdf](https://apps.who.int/iris/bitstream/handle/10665/331498/WHO-2019-nCoV-ICPPPE_use-2020.2-eng.pdf) (2020, accessed 3 August 2022).
4. Wang C and Otani Y. Removal of nanoparticles from gas streams by fibrous filters: A review. *Ind Eng Chem Res* 2013; 52: 15–17.
5. Adanur S. *Wellington Sears handbook of industrial textiles*. Technomic Publishing Co. Inc., Lancaster, Pennsylvania 1995.
6. Wang CS and Otani Y. Removal of nanoparticles from gas streams by fibrous filters: A review. *Ind Eng Chem Res* 2013; 52: 5–17.
7. Adanur S and Jayswal A. Filtration mechanisms and manufacturing methods of face masks: An overview. *J Ind Text* 2020; 51: 3683S–3717S.
8. Hill WC, Hull MS and MacCuspie RI. Testing of commercial masks and respirators and cotton mask insert materials using SARS-CoV-2 virion-sized particulates: Comparison of ideal aerosol filtration efficiency versus fitted filtration efficiency. *Nano Lett* 2020; 20: 7642–7647.
9. Mueller AV, Eden MJ, Oakes JM, et al. Quantitative method for comparative assessment of particle removal efficiency of fabric masks as alternatives to standard surgical masks for PPE. *Matter* 2020; 3: 950–962.
10. Blachere FM, Lemons AR, Coyle JP, et al. Face mask fit modifications that improve source control performance. *Am J Infect Control* 2022; 50: 133–140.
11. Whiley H, Keerthirathne TP, Nisar MA, et al. Viral filtration efficiency of fabric masks compared with surgical and N95 masks. *Pathogens* 2020; 9: 1–8.
12. Konda A, Prakash A, Moss GA, et al. Aerosol filtration efficiency of common fabrics used in respiratory cloth masks. *ACS Nano* 2020; 14: 6339–6347.
13. ASTM International. *F2299/F2299M – 03: Standard test method for determining the initial efficiency of materials used in medical face masks to penetration by particulates using latex spheres*, ASTM International, 100 Barr Harbor Drive, PO Box C700, West Conshohocken, PA 19428-2959, United States. 2017.
14. European Committee for Standardization. *EN 14683:2019+AC medical face masks – requirements and test methods*, CEN, Brussels, Belgium. 2019.
15. ASTM International. *F2101 – 19: Standard test method for evaluating the bacterial filtration efficiency (BFE) of medical face mask materials, using a biological aerosol of Staphylococcus aureus*, ASTM International, 100 Barr Harbor Drive, PO Box C700, West Conshohocken, PA 19428-2959, United States. 2019.
16. Whyte HE, Joubert A, Leclerc L, et al. Impact of washing parameters on bacterial filtration efficiency and breathability of community and medical facemasks. *Sci Rep* 2022; 12: 1–11.
17. Lou LH, Qin XH, and Zhang H. Preparation and study of low-resistance polyacrylonitrile nano membranes for gas filtration. *Text Res J* 2017; 87: 208–215.
18. Morris S, McAtee W, Capecelatro J, et al. Influence of expiratory flow pulsatility on the effectiveness of a surgical mask. *J Expo Sci Environ Epidemiol* 2022; 32: 697–705. <https://doi.org/10.1038/s41370-022-00416-x>
19. US FDA. N95 Respirators, surgical masks, face masks, and barrier face coverings, <https://www.fda.gov/medical-devices/personal-protective-equipment-infection-control/n95-respirators-surgical-masks-face-masks-and-barrier-face-coverings#s2> (2022, accessed 1 November 2022).
20. El-Atab N, Qaiser N, Badghaish H, et al. Flexible nanoporous template for the design and development of reusable anti-COVID-19 hydrophobic face masks. *ACS Nano* 2020; 14: 7659–7665.
21. Salvi SS. In this pandemic and panic of COVID-19 what should doctors know about masks and respirators?, <http://apiindia.org/wp-content/uploads/pdf/coronavirus/review-article-on-mask.pdf> (2020 accessed on 3 August 2022).
22. Derrick JL and Gomersall CD. Protecting healthcare staff from severe acute respiratory syndrome: Filtration capacity of multiple surgical masks. *J Hosp Infect* 2005; 59: 365–368.
23. Sandaradura I, Goeman E, Pontivivo G, et al. A close shave? Performance of P2/N95 respirators in healthcare workers with facial hair: Results of the BEARDS (BEnchmarking Adequate Respiratory DefenceS) study. *J Hosp Infect* 2020; 104: 529–533.
24. Smereka J, Ruetzler K, Szarpak L, et al. Role of mask/respirator protection against SARS-CoV-2. *Anesth Analg* 2020; 131: e33–e34.
25. Rengasamy S, Shaffer R, Williams B, et al. A comparison of facemask and respirator filtration test methods. *J Occup Environ Hyg* 2017; 14: 92–103.
26. Segovia JM, Huang CH, Mamishev M, et al. Performance of textile mask materials in varied humidity: Filtration efficiency, breathability, and quality factor. *Appl Sci (Basel)* 2022; 12: 9360.